British Journal of Pharmacology

DOI:10.1111/j.1476-5381.2011.01585.x
www.brjpharmacol.org

RESEARCH PAPER

Hyperphosphataemia sensitizes renally impaired rats to the profibrotic effects of gadodiamide

N Fretellier[1,5], JM Idée[1], P Bruneval[2,7], S Guerret[3], F Daubiné[4], G Jestin[1], C Factor[1], N Poveda[1], A Dencausse[1], F Massicot[5], O Laprévote[5,6], C Mandet[7], N Bouzian[1], M Port[1] and C Corot[1]

[1]*Guerbet, Research Division, Aulnay-sous-Bois, France,* [2]*Department of Pathology, Hôpital Européen Georges Pompidou, Paris, France,* [3]*Novotec, Lyon, France,* [4]*Atlantic Bone Screen, Nantes, France,* [5]*Chimie Toxicologie Analytique et Cellulaire, EA 4463, Faculté des Sciences Pharmaceutiques et Biologiques, Université Paris Descartes, Paris, France,* [6]*Service de Toxicologie Biologique, Hôpital Lariboisière, Paris, France, and* [7]*INSERM U970, Department of Pathology, Hôpital Européen Georges Pompidou, Paris, France*

Correspondence
Nathalie Fretellier, Guerbet, Research Division, BP 57400, Roissy Charles de Gaulle Cedex, France. E-mail: nathalie.fretellier@guerbet-group.com

Keywords
nephrogenic systemic fibrosis; hyperphosphataemia; renal impairment; gadolinium chelates; relaxometry; gadolinium; magnetic resonance imaging; contrast agents

Received
1 April 2011
Revised
20 June 2011
Accepted
27 June 2011

BACKGROUND AND PURPOSE
Hyperphosphataemia is common in patients with nephrogenic systemic fibrosis (NSF). NSF has been linked to administration of gadolinium (Gd) chelates (GCs) and elevated serum phosphate levels accelerate the release of Gd from linear, non-ionic GCs but not macrocyclic GCs. Hence, we determined whether hyperphosphataemia is a cofactor or risk factor for NSF by investigating the role of hyperphosphataemia in renally impaired rats.

EXPERIMENTAL APPROACH
Firstly, the clinical, pathological and bioanalytical consequences of hyperphosphataemia were investigated in subtotal nephrectomized (SNx) Wistar rats following i.v. administration of the non-ionic, linear GC gadodiamide (5 × 2.5 mmol·kg^{-1}·day^{-1}). Secondly, the effects of several GCs were compared in these high-phosphate diet fed rats. Total Gd concentration in skin, femur and plasma was measured by inductively coupled plasma mass spectrometry (ICP-MS) and free Gd^{3+} in plasma by liquid chromatography coupled to ICP-MS. Relaxometry was used to measure dissociated Gd in skin and bone.

KEY RESULTS
Four out of seven SNx rats fed a high-phosphate diet administered gadodiamide developed macroscopic and microscopic (fibrotic and inflammatory) skin lesions, whereas no skin lesions were observed in SNx rats treated with saline, the other GCs and free ligands or in the normal diet, gadodiamide-treated group. Unlike the other molecules, gadodiamide gradually increased the r_1 relaxivity value, consistent with its *in vivo* dissociation and release of soluble Gd.

CONCLUSIONS AND IMPLICATIONS
Hyperphosphataemia sensitizes renally impaired rats to the profibrotic effects of gadodiamide. Unlike the other GCs investigated, gadodiamide gradually dissociates *in vivo*. Our data confirm that hyperphosphataemia is a risk factor for NSF.

Abbreviations
α-SMA, α-smooth muscle actin; DTPA, diethylene triamine pentaacetic acid; EC, endothelial cells; ECM, extracellular matrix; Gd, gadolinium; GC, gadolinium chelates; HPLC, high performance liquid chromatography; ICP-MS, inductively coupled plasma mass spectrometry; MRI, magnetic resonance imaging; NSF, nephrogenic systemic fibrosis; P-4-OH, prolyl-4-hydroxylase; SNx, subtotal nephrectomy; TIMP-1, tissue inhibitor of metalloproteinase-1; DOTA, 1,4,7,10-tetraazacyclododecane-N,N′,N′,N″-tetraacetic acid

Introduction

Nephrogenic systemic fibrosis (NSF) is a rare and highly debilitating systemic fibrosing disorder occurring in patients with severe or end stage renal failure, usually those requiring dialysis (Cowper *et al.*, 2001). NSF is typically characterized by extensive thickening and hardening of the skin associated with contractures around the joints impairing mobility, pruritus and sharp pain. Histologically, NSF is characterized by dermal fibrosis with CD34 and procollagen 1-positive cells, prominent collagen bundles, frequent presence of myxoid substance between fibroblasts and collagen bundles, and increased numbers of macrophages and factor XIIIa-positive dendritic cells (Braverman and Cowper, 2010).

The link between administration of gadolinium (Gd) chelates (GCs), used as contrast agents for magnetic resonance imaging (MRI), and the disease, suggested for the first time in 2006 (Grobner, 2006), is now acknowledged. Briefly, there are two structurally distinct categories of GCs: (i) 'macrocyclic' molecules in which the Gd^{3+} ion is 'caged' into the pre-organized cavity of the ligand; and (ii) 'linear' chelates in which the ligand is wrapped around the metal ion. GCs can also be either 'non-ionic' (in which case three carboxylate functions neutralize the three positive charges of Gd^{3+}) or 'ionic' (where additional carboxylic acid groups are salified with either meglumine or sodium) (Port *et al.*, 2008). GCs differ in terms of their thermodynamic and kinetic stabilities. High kinetic stability provided by the macrocyclic structure combined with high thermodynamic stability minimize the amount of free Gd^{3+} that can be released from the parent chelate (Port *et al.*, 2008). Virtually all published cases of NSF have been associated with prior administration of linear GCs (Broome, 2008; Perazella and Reilly, 2011).

The mechanism of NSF is not fully understood despite extensive research (Vakil *et al.*, 2009; Varani *et al.*, 2009; Edward *et al.*, 2010). Clinically relevant preclinical models are needed to more clearly understand the mechanism of this disease. Rats submitted to subtotal (5/6) nephrectomy (SNx) have been widely used as a model of NSF (Grant *et al.*, 2009; Pietsch *et al.*, 2009; Haylor *et al.*, 2010; Fretellier *et al.*, 2011a). Overall, these studies concluded that fibrotic-like lesions can be induced in rats treated with the linear GC gadodiamide.

Elevated plasma phosphate levels have been shown to accelerate the release of free Gd^{3+} from linear, non-ionic GCs such as gadodiamide, whereas macrocyclic GCs remained stable in human serum at both normal and high phosphate levels (Frenzel *et al.*, 2008). As higher serum phosphate levels have been reported in patients with nephrogenic systemic fibrosis compared with sex- and age-matched renal failure control patients (Marckmann *et al.*, 2007), the purpose of the present study was to: (i) investigate the clinical and pathological consequences of hyperphosphataemia in renally impaired rats following administration of the linear, non-ionic GC gadodiamide; and (ii) compare the clinical and biochemical effects of all categories of GCs and free ligands on SNx rats fed a high-phosphate diet and the possibility of *in vivo* dissociation of GCs, by using the relaxometry method (Fretellier *et al.*, 2011b).

Our data indicate that hyperphosphataemia sensitizes renally impaired rats to the profibrotic effects of the linear and non-ionic GC gadodiamide. No effects were observed for the other categories of GCs and the free ligands Ca-DOTA and Ca-DTPA. In gadodiamide-treated rats, increased r_1 relaxivity values were found in both femur and skin. These results indicate gradual *in vivo* dissociation of gadodiamide, whereas the other GCs remained stable.

Methods

Animals

All studies were carried out on male Wistar rats from Centre d'Elevage René Janvier (CERJ) (Le Genest Saint-Isle, France), aged 6 weeks and weighing 170 ± 7 g. The animals underwent one-step subtotal (5/6) nephrectomy performed at CERJ: animals were anaesthetized with ketamine (100 mg·kg^{-1}) and xylazine (10 mg·kg^{-1}). The right kidney was exposed via a flank incision, the adrenal gland was separated from the upper pole and the kidney was decapsulated. The renal pedicle was ligated and the right kidney was removed. The left kidney was subsequently decapsulated and the adrenal gland was separated from the upper pole. Ligatures were placed around the upper and lower poles and the poles were then excised. An intravenous injection of 1.0 mL·kg^{-1} of saline was performed at completion of surgery to compensate for blood loss. The animals were housed one per cage at an ambient temperature of 22 ± 2°C, hygrometry of 45 ± 10%, with 12/12 light/dark cycles. Animals had free access to water and animal chow.

All animal care and experimental procedures were carried out according to French regulations and in compliance with the European Economic Community Directive (2010/63/EU) on animal welfare. The protocol was approved by the local ethics committee.

Role of hyperphosphataemia (Study 1)

Male Wistar rats subjected to subtotal (5/6) nephrectomy (n = 7 to 8/group) received a normal phosphate (0.6%) diet or a high-phosphate (1.1%) diet and were allocated to single daily i.v. injections of 2.5 mmol·kg^{-1} (5.0 mL·kg^{-1}) of gadodiamide or saline (5.0 mL·kg^{-1}) for 5 consecutive days, starting 10 days after subtotal nephrectomy. The 1.1% phosphate diet was given to rats throughout their lifespan, including *in utero* period as their mothers were fed with this diet from the 11th day of gestation. For Gd measurement, a skin biopsy was performed on Day 4 after the first administration, with a biopsy punch (6 mm diameter) and the wounds were then sutured. The rats were killed (exsanguination under isoflurane anaesthesia) 11 days after the first administration. All injections and skin samples were performed under isoflurane/oxygen (3.5% induction, then 2.5%, 1 L·min^{-1} oxygen) anaesthesia.

Comparison of various GCs and ligands in SNx and rats fed a high-phosphate diet (Study 2)

Male Wistar rats subjected to subtotal (5/6) nephrectomy (n = 6 to 8/group) received a high-phosphate (1.1%) diet and were allocated to single daily i.v. injections of 2.5 mmol·kg^{-1} of gadoterate, gadodiamide, gadobenate, gadobutrol or 0.5 mmol·kg^{-1} of the ligands Ca-DTPA or Ca-DOTA or saline

used as control (5.0 mL·kg^{-1}) for 5 consecutive days, starting 10 days after subtotal nephrectomy. Skin biopsies were performed on Days 1 and 8 after the first administration. The rats were killed 25 days after the first administration.

Macroscopic skin findings and histopathology

All rats were examined for macroscopic skin changes before the first injection and then daily throughout the study. Skin biopsy samples were fixed in 4% neutral buffered formalin. After routine dehydration, the samples were embedded in paraffin, sectioned (5 µm thickness) and stained by haematoxylin-eosin-saffron staining for histopathological analysis (Studies 1 and 2), picrosirius red to detect the presence of collagen (Study 1) and Alcian blue for acidic mucopolysaccharides (Study 1).

Immunohistochemical staining was performed in both studies to detect CD34 and TGFβ$_1$ using anti-CD34 goat antibody (diluted to 1:1000, R&D Systems, Minneapolis, MN, USA) and anti-TGFβ$_1$ rabbit antibody (diluted to 1:250, GeneTex, San Antonio, TX, USA) using ImmPRESS polymerized reporter peroxidase staining (ImmPRESS anti-goat Ig [peroxidase] kit [MP 7405] and ImmPRESS anti-rabbit Ig [peroxidase] kit [MP 7401], respectively; Vector Laboratories Burlingame, CA. USA).

In Study 2, in addition to CD34 and TGFβ1, immunostaining of S100A4 (i.e. fibroblast-specific protein-1) (rabbit antibody diluted to 1:500, Abcam, Paris, France), using anti-rabbit biotinylated antibody (AbCys, Paris, France) staining, α-smooth muscle actin (α-SMA) (mouse antibody diluted to 1:600, Thermo Fisher Scientific, Brebières, France) using anti-mouse biotinylated antibody (AbCys) staining, macrophages (ED-1 stain) (mouse antibody diluted to 1:100, AbD Serotec, Colmar, France) using anti-mouse biotinylated antibody (AbCys) staining, tissue inhibitor of metalloproteinase-1 (TIMP-1) (goat antibody diluted to 1:100, R&D Systems, Minneapolis, MN, USA) using anti-goat biotinylated antibody (AbCys) staining and prolyl-4-hydroxylase (P-4-OH) (mouse antibody diluted to 1:100, Acris Antibodies GmbH, Herford, Germany) using anti-mouse biotinylated antibody (AbCys) staining, was performed at the end of the study. Histopathological lesions were evaluated semi-qualitatively using a 4-point severity grading scale (– absent; ± mild; + moderate; ++ severe) for each animal. Histopathological examinations were performed in a blinded fashion by certified histopathologists (S. G. in Study 1 and P. B. in Study 2) in accordance with the guidelines of the Society of Toxicological Pathology (Crissman *et al.*, 2004).

Biochemistry

In Study 2, the plasma levels of total calcium, phosphorus, transferrin-bound iron and creatinine (Vitros-II autoanalyzer, OrthoClinical Diagnostics Inc., Issy-les-Moulineaux, France) were measured on Days 0 (i.e. 3 days before the first administration), 5 and 25. In addition, plasma levels of monocytes chemotactic protein-1 (MCP-1) (Bender MedSystems, Vienna, Austria), TIMP-1 and TGFβ$_1$ (R&D Systems, Minneapolis, MN, USA) were measured by ELISA on Day 5. Plasma levels of TGFβ$_1$ and fibroblast growth factor-23 (Kainos Laboratories, Tokyo, Japan) were measured by ELISA on Day 25. Blood samples were taken from the sublingual vein (Mahl *et al.*, 2000). All assays were performed in duplicate.

Gadolinium determination

In Study 2, Gd levels in plasma, skin, liver and femoral epiphyseal samples, were measured by inductively coupled plasma mass spectrometry (ICP-MS) on ELAN DRC Plus® (PerkinElmer Life and Analytical Sciences, Inc., Waltham, MA, USA). A standard curve of inorganic Gd (0.64 nmol·L^{-1} to 1.30 µmol·L^{-1}) in 6.5% HNO_3 was used by monitoring the signal of the ^{157}Gd isotope. The acceptance limits (total error) were set at ±14%. Results are expressed in nmol Gd·g^{-1} wet tissue weight (tissues samples) or µmol·L^{-1} of plasma. The limit of quantification was 0.64 nmol·L^{-1}. Samples above the limit of detection (0.19 nmol·L^{-1}) but below the limit of quantification were given an arbitrary value of 0.32 nmol·L^{-1}. The dissociated Gd^{3+} concentration was measured by high performance liquid chromatography (HPLC) connected to an ICP-MS system as described elsewhere (Fretellier *et al.*, 2011b).

Relaxometry measurements

In Study 2, the presence of dissociated Gd in skin biopsies and trabecular femur was assessed by relaxometry technique because mass spectrometry cannot characterize the exact nature of Gd species in solid tissues. This technique has been described elsewhere (Fretellier *et al.*, 2011b). Briefly, the samples were mashed, differently according to the matrix, and were diluted (1/11) in D_2O/H_2O (90/10) mix. Longitudinal relaxation times (T1) were measured on Bruker Minispec (Bruker Optics, Ettlingen, Germany) at 60 MHz (i.e. 1.42 T) and 37°C.

The r_1 relaxivity value could not be determined when the $1/T1_{sample} - 1/T1_{diamagnetic}$ value was less than 20% of $1/T1_{diamagnetic}$ in the absence of Gd precipitation (i.e. because of a low total Gd concentration in the sample). The Gd concentration was then determined by ICP-MS. The Gd concentration in tissue samples was corrected for an estimated 97% water content, based on unpublished in-house studies. Relaxivities (r_1 apparent value) were calculated according to the formula: $r_1 = (1/T1_{sample} - 1/T1_{diamagnetic})/[Gd]$, where relaxation rate (1/T1) was expressed in s^{-1}, Gd concentration in mM and relaxivity r_1 in mM^{-1}·s^{-1}.

Relaxometry studies (*in vitro* spiking studies) on biological matrices were performed by spiking with GC (from commercial solutions) (range of 0, 0.005, 0.01, 0.02, 0.04, 0.05, 0.1, 0.5 and 1 mM) on D_2O/H_2O mix, rat plasma, skin and trabecular femur from untreated rats. The term '*in vitro* studies' refers to all experiments performed by spiking GC on tissue matrices (to obtain the reference range of r_1 relaxivities) and '*in vivo* studies' refers to all experiments performed on test animals. Based on unpublished *in vitro* relaxometry studies, the uncertainty of relaxivity r_1 measurements (with Gd concentration measured by ICP-MS) was set at r_1 ±23%. The *in vitro* r_1 relaxivity range represents the *in vitro* r_1 relaxivity value (obtained from spiking studies) ± uncertainty of 23%.

Statistical analysis

Data are expressed as mean ± SD. Statistical analysis was carried out using GraphPad Prism 4 (GraphPad Software Inc, San Diego, CA, USA). Results were analysed by repeated-

measures ANOVA (body weight, biochemistry data, plasma Gd concentration) or by one-way ANOVA (Gd concentrations) followed, when relevant, by a Bonferroni or Dunnett's test. Skin relaxivity values were analysed by Student's *t*-test. Differences were considered significant when $P < 0.05$.

Materials

Meglumine gadoterate (Dotarem, batch 09GD022A, Guerbet, Villepinte, France), gadodiamide (Omniscan, batch 10758384 and batch 10942539, General Electrics Healthcare, Chalfont St Giles, UK), dimeglumine gadobenate (MultiHance, batch S9P252A, Bracco, Milan, Italy), gadobutrol (Gadovist, batch 9A033A, Bayer Healthcare, Berlin, Germany) were purchased from respective manufacturers. The ligands Ca-DTPA (diethylene triamine pentaacetic acid) and Ca-DOTA (1,4,7, 10-tetraazacyclododecane-N,N′,N′,N″-tetraacetic acid) were synthesized at Guerbet Research Dpt. Saline was purchased from Lavoisier (Paris, France).

Results

Characterization of the experimental model

An increase in plasma creatinine (66.8 ± 20.1 vs. 25.8 ± 2.1 $\mu mol \cdot L^{-1}$, $P < 0.01$) and phosphorus (3.4 ± 0.8 vs. 2.0 ± 0.1 $mmol \cdot L^{-1}$, $P < 0.01$) levels was observed in SNx rats fed the high-phosphate diet compared with sham operated rats. Plasma calcium levels remained unchanged (2.1 ± 0.2 vs. 2.4 ± 0.1 $mmol \cdot L^{-1}$, not significant). Pathological lesions consistent with osteodystrophy (osteitis fibrosa) were found in both the femur and tibia of SNx rats fed a high-phosphate diet (data not shown).

Role of hyperphosphataemia (Study 1)

Macroscopic and microscopic findings. The plasma phosphate level was higher in SNx rats receiving a high-phosphate diet than in SNx rats fed a normal diet (2.4 ± 0.4 and 1.9 ± 0.2 $mmol \cdot L^{-1}$, respectively; $P < 0.05$). Plasma calcium levels were similar in the two groups (2.2 ± 0.2 and 2.3 ± 0.2 $mmol \cdot L^{-1}$, respectively; not significant). No skin lesions were observed in the gadodiamide- and saline-treated groups receiving a normal-phosphate diet, while four out of the seven gadodiamide-treated rats fed a high-phosphate diet showed macroscopic skin lesions (ulcerations and scabs) in the neck, back and abdominal skin for the first time on Day 8 (i.e. after the first injection). No significant differences in body weight changes were observed between these groups.

Histologically, small superficial epidermal lesions, degradation and merging of collagen fibres in the dermis with disorganization of the extracellular matrix (ECM) were observed in the gadodiamide group fed with normal diet, while numerous zones of epidermal necrosis, a moderately increased dermal cellularity, the presence of multinucleated giant cells, more abnormalities of dermal collagen structures (dense and short collagen bundles alternating with altered collagen fibres) and more intense $TGF\beta_1$ immunostaining were observed in the gadodiamide-treated rats fed a high-phosphate diet (Figure 1).

Comparison of various GCs and ligands in rats fed a high-phosphate diet (Study 2)

Macroscopic and microscopic findings. Ulcerative and squamous skin eruptions occurred (from Day 8 until Day 23) in five of the eight rats receiving gadodiamide, and worsened in four animals or improved in one, while no skin lesions were observed in the rats treated with saline, the other GCs and the free ligands. Four gadodiamide-treated rats had to be killed for ethical reasons because of the severity of the skin lesions and loss of body weight (one rat was killed at Day 5, one at Day 15, one at Day 22 and one at Day 23). No scratching was observed. One gadoterate-treated rat was found dead at Day 8. No significant differences in body weight changes were observed between these groups.

On histological examination, the skin was considered to be abnormal in six of the eight rats of the gadodiamide-treated group (three rats with macroscopic skin lesions and killed, one rat without macroscopic skin lesions and killed and two rats without skin lesions and not killed before the end of the experiment), while no histological skin changes were observed in the other groups. Lesions consisted of bands of inflammatory dermal fibrosis associated with hyperkeratosis and calcifications (Figure 2). ED-1, TIMP-1 and $TGF\beta_1$-positive macrophages accumulated in the dermis (Figure 2, Table 1) and were associated with an increased density of CD34+ and S100A4+ spindle cells. Positive immunostaining for $TGF\beta_1$, TIMP-1 and P-4-OH (Figure 2) was observed for spindle cells of gadodiamide-treated rats (6/8). No α-smooth muscle actin expression was detected, irrespective of the group. In all other groups and in the controls, immunohistochemical patterns were normal except for one rat treated with gadobenate, in which a fibro-inflammatory focus located in the dermis with the presence of ED-1 and $TGF\beta_1$-positive cells was observed.

Biochemistry. No significant differences between the groups were found regarding the plasma levels of all tested parameters at Day 0. The plasma creatinine level of all treated-groups was consistent with renal impairment (data not shown). A slight and non-significant decrease in plasma phosphorus levels was observed from Day 5 in the gadodiamide, gadobutrol, gadobenate and Ca-DOTA-treated groups (Table 2). A substantial decrease in plasma phosphorus levels (–30%) was observed at Day 5 in the Ca-DTPA-treated group ($P < 0.05$ vs. Day 0 values).

A slight and non-significant increase in plasma iron concentration was also observed on Day 5 in saline, gadoterate, gadobutrol and Ca-DOTA-treated groups. Because analytical interference of iron measurement was observed with Ca-DTPA, gadobenate and gadodiamide, no results are provided for these compounds (Table 2).

No significant differences in plasma levels of $TGF\beta_1$ and fibroblast growth factor-23 were observed between the various groups (data not shown). The GCs and ligands had no effect on plasma levels of MCP-1 and TIMP-1 (measured on Day 5) (data not shown). However, an increase in the plasma levels of MCP-1 (17 times vs. controls) and TIMP-1 (seven times vs. controls) was observed in one gadodiamide-treated rat (this animal was killed at Day 5).

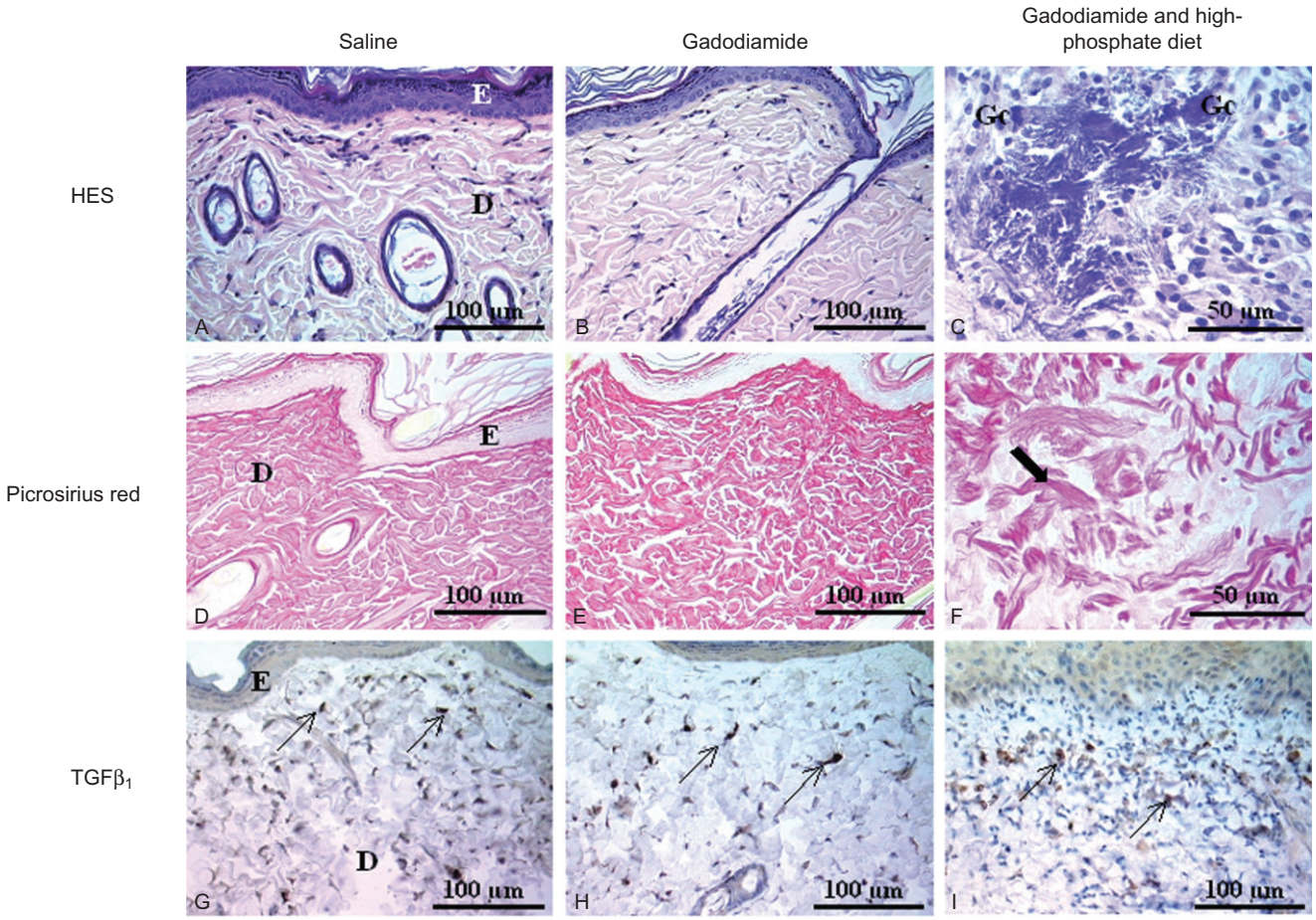

Figure 1

Histological skin lesions in the papillary dermis: haematoxylin and eosin staining (A–C) to analyse cellular lesions, picrosirius red staining (D–F) to detect changes in extracellular matrix and TGFβ$_1$ (G–I) to detect spindle cells (Study 1). Saline (A, D, G): epidermal thickness was constant; the dermis was weakly cellular, and ECM was homogeneous. TGFβ$_1$ was only expressed on several spindle cells. Gadodiamide (B, E, H): local epidermal necrosis and presence of some inflammatory cells in the papillary (or superficial) dermis. ECM was heterogeneous, with small clusters of collagen fibres. TGFβ$_1$ immunohistochemical detection was slightly increased in papillary and reticular dermis. Gadodiamide in SNx rats fed a high-phosphate diet (C, F, I): numerous foci of epidermal necrosis; some foci of myxoid tissue, necrosis, presence of multinucleated giant cells, [Gc] included in fragmented collagen fibres, were observed (C, F), as well as an increase in subepithelial TGFβ$_1$ immunostaining (I). (F) Shows short and dense collagen bundles alternating with altered fibres. D, dermis; E, epidermis; HES, haematoxylin-eosin-saffron.

Plasma levels of total and dissociated gadolinium. No significant differences in plasma total Gd levels were observed in the gadoterate, gadodiamide or gadobutrol-treated groups (Figure 3), while plasma total Gd levels were lower with gadobenate than with the other GCs ($P < 0.05$ at Day 8). No dissociated Gd^{3+} was found in the plasma of gadobutrol and gadobenate-treated rats, regardless of the time-point, while two rats (out of eight) showed the presence of Gd^{3+} levels at Day 8 in the gadoterate treated-group (Table 3). Marked release of Gd^{3+} was observed with gadodiamide in all treated animals (Table 3).

Total gadolinium levels in skin. No significant differences in total Gd concentration in skin at Day 8 were observed between treated groups except for gadobenate-treated rats, in which the Gd concentration was significantly lower than in the other groups (Figure 4). A dramatic decrease in the skin total Gd concentration at Day 25 (vs. Day 8) (Figure 4) was observed in the gadoterate, gadobutrol and gadobenate-treated groups. The total Gd concentration in dorsal skin was higher ($P < 0.001$) with gadodiamide (153.0 ± 82.7 nmol·g^{-1}) than in the other GC-treated groups at Day 25.

Total gadolinium levels in the femur and liver. Total Gd concentrations in the femur and liver were higher in the gadodiamide-treated group than in the other treated groups ($P < 0.001$) (Figure 5A and B).

Relaxometry studies. The r_1 relaxivity values obtained in water (90/10 D_2O/H_2O solution), rat skin, femur, plasma and liver matrices (*in vitro* 'spiking' studies) are shown in Table 4.

In *in vivo* studies, the r_1 relaxivity values of gadoterate or gadobutrol were situated in the r_1 *in vitro* range in skin (Days 1 and 8) and femur (Figures 6 and 7). However, in 19/25 rats

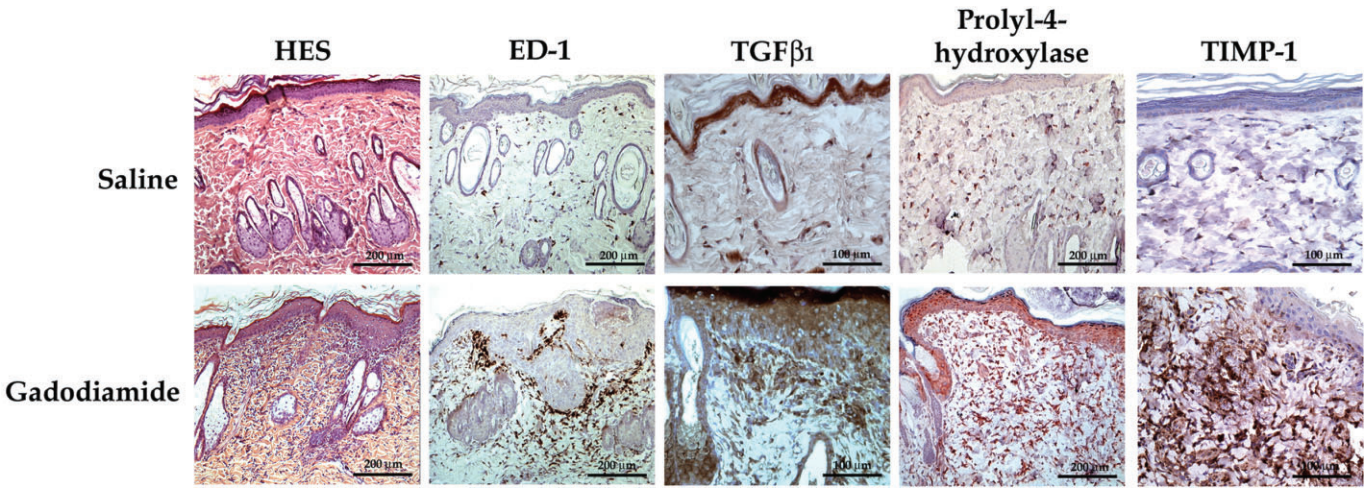

Figure 2

Histological (haematoxylin-eosin-saffron [HES]), and immunohistochemical (ED-1, TGFβ_1, prolyl-4-hydroxylase, TIMP-1) analysis of dorsal skin in SNx rats fed a high-phosphate diet (typical examples from Study 2). Bands of inflammatory dermal fibrosis associated with hyperkeratosis and calcifications were observed (HES) as well as the presence of ED-1 + macrophages, TGFβ_1, prolyl-4-hydroxylase and TIMP-1 immunostaining in the dermis.

Table 1

Semi-quantitative immunohistochemical analysis of dorsal skin (number of rats with positive immunostaining)

Treatment	No of rats	CD34	ED-1	TGFβ1	S100A4	α-SMA	P-4-OH	TIMP-1
Saline	5	(+) [sc and ECs]	(±)	(–)	(+) [sc]	(–)	(±)	(±)
Gadoterate	8	(+) [sc and ECs]	(±)	(–)	(+) [sc]	(–)	(±)	(±)
Gadodiamide	8	(+) [sc and ECs] but ↑ number of sc	(±) = 3 (++) = 5	(–) = 2 (foci) = 2 (+) = 1 (++) = 3	(+) [sc] but ↑ number of sc	(–)	(±) = 2 Foci (++) = 6	(±) = 2 Foci (++) = 6
Gadobenate	7	(+) [sc and ECs]	(±) = 6 (++) = 1 (focus)	(–) = 6 (++) = 1 (focus)	(+) [sc]	(–)	(±)	(±)
Gadobutrol	7	(+) [sc and ECs]	(±)	(–)	(+) [sc]	(–)	(±)	(±)
Ca-DOTA	6	(+) [sc and ECs]	(±)	(N/A)	(N/A)	(N/A)	(N/A)	(N/A)
Ca-DTPA	6	(+) [sc and ECs]	(±)	(N/A)	(N/A)	(N/A)	(N/A)	(N/A)

'sc' indicates spindle cells and 'ECs' indicates endothelial cells. – = absence, ± = mild, + = moderate, ++ = severe, N/A = not available.

(gadoterate, gadobutrol and gadobenate), the r_1 value could not be determined at Day 25 because the $1/T1_{sample} - 1/T1_{diamagnetic}$ value was less than 20% of $1/T1_{diamagnetic}$ (low total Gd concentration in the samples). A slight and non-significant increase in the r_1 value was observed at Day 8 (vs. Day 1 value) in skin samples from gadobenate-treated rats.

A gradual increase in the r_1 relaxivity value ($P < 0.01$ at Day 8 vs. Day 1 and $P < 0.05$ at Day 25 vs. Day 1) was observed in the dorsal skin of gadodiamide-treated rats (Figure 6).

In the gadodiamide (all rats) and gadobenate ($n = 2$ measurable) groups, the r_1 value exceeded the r_1 *in vitro* range in femur samples (Figure 7). A dramatic increase in the *in vivo* r_1 relaxivity value (38.2 ± 10.4 $mM^{-1}{\cdot}s^{-1}$) was observed in the liver in the gadobenate-treated group, compared with the *in vitro* r_1 relaxivity value (4.9 $mM^{-1}{\cdot}s^{-1}$).

Discussion and conclusions

Most patients with end-stage renal failure present hyperphosphataemia, which is associated with secondary hyperparathyroidism, osteodystrophy and increased mortality (Coladonato, 2005). In two case-control studies, significantly higher serum phosphate levels were observed in NSF patients, compared with patients with chronic kidney disease but with

Table 2

Plasma phosphorus or iron levels on Day 0 and percentage change (%) of plasma phosphorus or iron levels compared with Day 0

Treatment	Phosphorus Plasma (phosphorus) ($mmol \cdot L^{-1}$) Day 0	Percentage change versus Day 0 (%) Day 5	Day 25	Iron Plasma (iron) ($\mu mol \cdot L^{-1}$) Day 0	Percentage change versus Day 0 (%) Day 5	Day 25
Saline	3.3 ± 0.8	–5	–10	43.4 ± 15.6	+12	–2
Gadoterate	3.0 ± 0.2	+6	–1	42.1 ± 7.2	+21	+18
Gadodiamide	3.1 ± 0.3	–7	–13	37.1 ± 8.3	§	§
Gadobutrol	2.7 ± 0.4	–8	–15	43.8 ± 9.5	+5	+3
Gadobenate	2.8 ± 0.5	–13	–15	47.8 ± 9.8	§	§
Ca-DOTA	2.8 ± 0.3	–8	–15	33.5 ± 6.0	+18	+3
Ca-DTPA	2.8 ± 0.2	–30*	–13	37.8 ± 8.6	§	§

*$P < 0.05$ versus control (saline) group.
§Analytical interference. Uninterpretable data.

Table 3

Dissociated Gd concentration in plasma on Day 8 and Day 15 (HPLC-ICP-MS) and dissociated/total Gd concentration ratio

Treatment	Day 8 Dissociated [Gd^{3+}] in plasma ($\mu mol \cdot L^{-1}$)	Dissociated/total Gd concentration ratio (%)	Day 15 Dissociated [Gd^{3+}] in plasma ($\mu mol \cdot L^{-1}$)	Dissociated/total Gd concentration ratio (%)
Gadoterate	<LOD ($n = 6$) 1.1 ($n = 2$)	36 ($n = 2$)	<LOD ($n = 7$)	–
Gadodiamide	2.4 ± 0.9 ($n = 7$)	71 ± 23 ($n = 7$)	<LOD ($n = 3$) 1.3 ± 0.9 ($n = 4$)	110 ± 10 ($n = 4$)
Gadobutrol	<LOQ ($n = 7$)	–	<LOD ($n = 4$) <LOQ ($n = 3$)	–
Gadobenate	<LOQ ($n = 7$)	–	<LOD ($n = 1$) <LOQ ($n = 6$)	–

LOD indicates limit of detection and LOQ indicates limit of quantification.

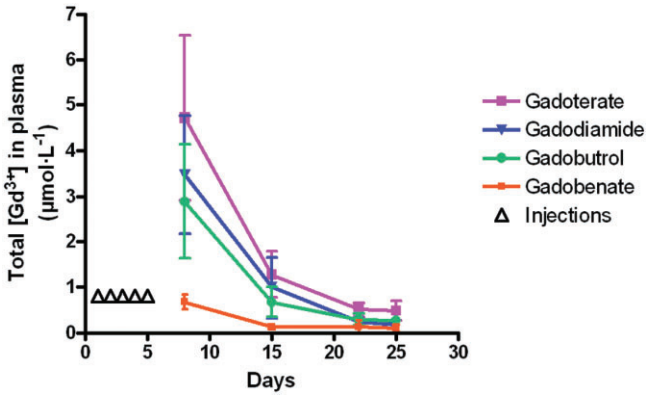

Figure 3

Total Gd concentration measured in plasma of rats subjected to subtotal nephrectomy and high-phosphate diet receiving each GC (5 × 2.5 $mmol \cdot kg^{-1}$ IV) (ICP-MS measurement) between Day 8 and Day 25. *$P < 0.05$ versus other GCs.

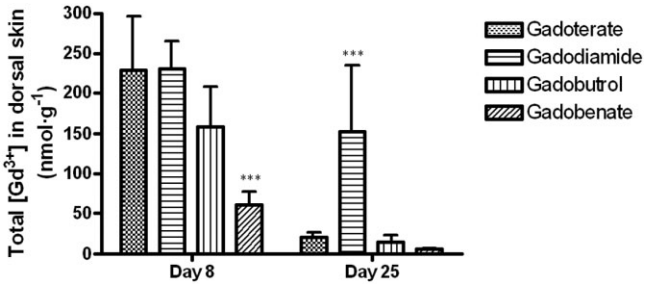

Figure 4

Total Gd concentration measured in skin samples of rats subjected to subtotal nephrectomy and high-phosphate diet receiving each GC (5 × 2.5 $mmol \cdot kg^{-1}$ IV) on Day 8 and Day 25 (rat killed) (ICP-MS measurement). In untreated rats (control group), the total Gd concentration in skin was 1.9 ± 1.3 $nmol \cdot g^{-1}$ on Day 8 and 1.7 ± 1.4 $nmol \cdot g^{-1}$ on Day 25. ***$P < 0.001$ versus all GC treated-groups.

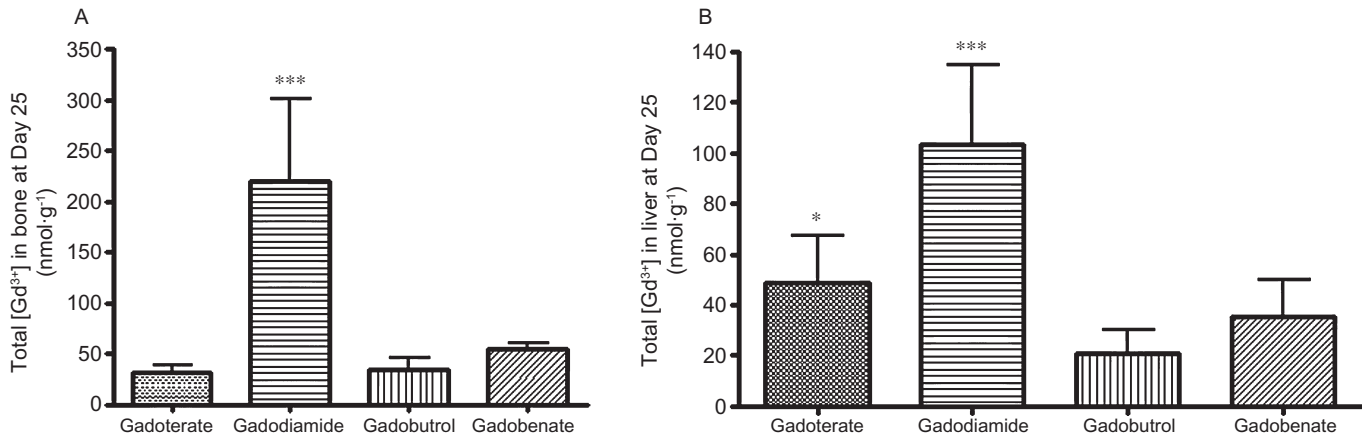

Figure 5

Total Gd concentration measured in bone (A) or in liver (B) samples of SNx rats fed a high-phosphate diet receiving each GC (5×2.5 mmol·kg^{-1} i.v.) on Day 25 (rat killed) (ICP-MS measurement). In untreated rats (control group), the total Gd concentration was 0.8 ± 1.2 nmol·g^{-1} in bone samples and below the limit of quantification in liver samples. ***$P < 0.001$ versus all GC-treated groups. *$P < 0.05$ versus gadobutrol.

Table 4

In vitro r_1 relaxivity value (spiking studies with gadoterate, gadodiamide, gadobutrol or gadobenate [60 MHz, 37°C]) in D_2O/H_2O and various tissue matrices from control rats

Matrix	*In vitro* r_1 relaxivity ($mM^{-1}·s^{-1}$) (±23%) Gadoterate	Gadodiamide	Gadobutrol	Gadobenate
D_2O/H_2O (90/10)	3.3 [2.5–4.1]	3.7 [2.9–4.6]	3.8 [2.9–4.7]	4.8 [3.7–5.9]
Trabecular Femur	3.8 [2.9–4.7]	4.6 [3.5–5.7]	4.5 [3.5–5.6]	4.6 [3.5–5.7]
Dorsal skin	3.0 [2.3–3.7]	4.5 [3.5–5.6]	3.5 [2.7–4.3]	4.8 [3.7–5.9]
Plasma	3.7 [2.9–4.6]	4.1 [3.2–5.0]	4.4 [3.4–5.4]	5.7 [4.4–7.0]
Liver	–	–	–	4.9 [3.7–5.9]

The uncertainty of relaxivity r_1 measurements (Gd concentration measured by ICP-MS) was set at r_1 ±23%.

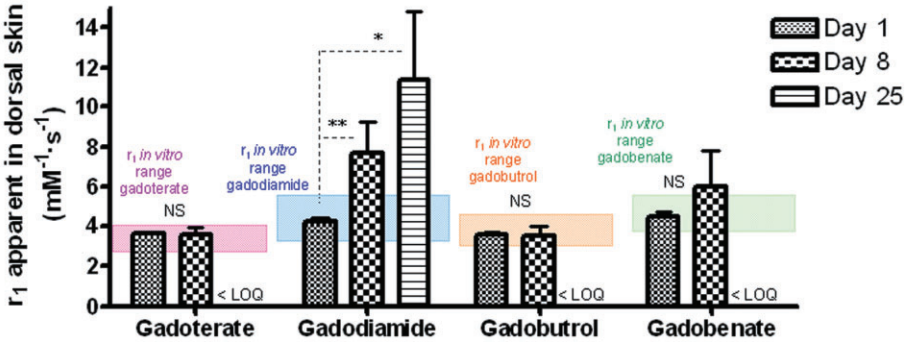

Figure 6

Relaxivity r_1 values (60 MHz, 37°C) in skin samples of SNx rats fed a high-phosphate diet treated with gadoterate, gadodiamide, gadobutrol or gadobenate on Days 8 and 25 (rat killed). *$P < 0.05$ versus gadobenate and gadobutrol. **$P < 0.01$ versus all GC-treated groups. LOQ indicates limit of quantification. NS, not significant.

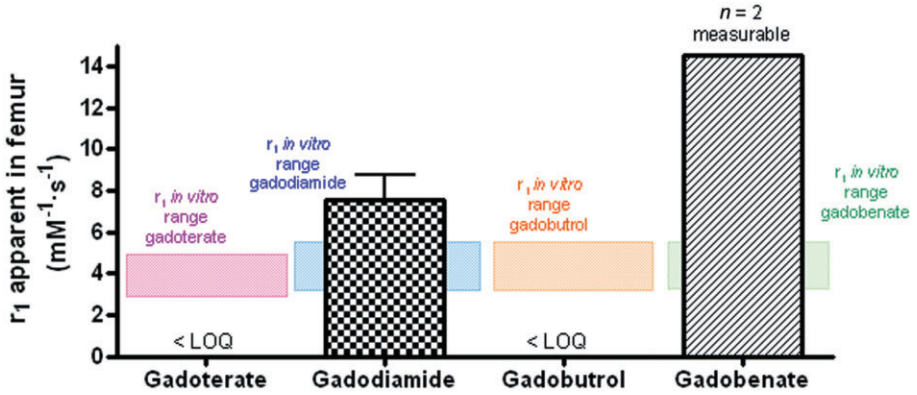

Figure 7

Relaxivity r_1 values (60 MHz, 37°C) in (trabecular) bone samples of SNx rats fed a high-phosphate diet treated with gadoterate, gadodiamide, gadobutrol or gadobenate on Day 25 (rat killed). LOQ indicates limit of quantification.

no signs of NSF (Marckmann *et al.*, 2007; Prince *et al.*, 2008). The main purpose of our study was to determine whether hyperphosphataemia is a cofactor or a risk factor of NSF as suggested by Peak and Sheller (2007).

The GC administration protocol used in our studies is similar to that used by other teams (Grant *et al.*, 2009; Pietsch *et al.*, 2009). Although the dose used was higher than the range 0.1 to 0.3 mmol·kg^{-1} used for MRI contrast examination in clinical practice, it is appropriate for chronic studies in the rat because the comparative drug doses between species should be normalized to body surface area rather than body weight (US Food and Drugs Administration CfDEaR, 2005).

The SNx and high-phosphate diet rat model used in this study is classically used as a model of hyperparathyroidism (Sanchez *et al.*, 2004; Jiang and Wang, 2008) and bone lesions (Oste *et al.*, 2007). Both the bioavailability of phosphorus and the degree of renal failure are important parameters in the clinical relevance of the SNx rat model-associated osteodystrophy (Oste *et al.*, 2007). Phosphorus sources in the standard rat diet present a low bioavailability. However, the high-phosphate diet used in this study included inorganic Ca/P sources (monocalcium phosphate) with a high absorption rate, leading to a high bioavailability of phosphorus (Oste *et al.*, 2007).

In the first study, histological lesions consistent with those observed in NSF patients, including a haphazard arrangement of short and dense collagen bundles (Cowper *et al.*, 2008; Braverman and Cowper, 2010) were observed in SNx rats fed a high-phosphate diet and treated with gadodiamide. Multinucleated giant cells were observed, a feature sometimes reported in NSF patients (Wilford *et al.*, 2010). Gadodiamide-induced fibrosis-like lesions were more marked in SNx rats fed a high-phosphate diet than in SNx rats fed with normal diet. It has been shown (Fretellier *et al.*, 2011a) that no dermal fibrosis was observed up to 32 days after the first injection of gadodiamide, thus ruling out the possibility that high-phosphate diet may have accelerated the response. Epidermal lesions were also found in gadodiamide-treated SNx rats fed a high-phosphate diet. However, in rats, microscopic dermal abnormalities should be considered to be more clinically relevant than macroscopic epidermal lesions (e.g. scabs). Thus, in addition to impaired renal function, hyperphosphataemia sensitizes the model. These data are therefore consistent with the role of hyperphosphataemia as a risk factor rather than a cofactor in NSF.

In the second study, all chemical categories of GCs and two polyazapolycarboxylic ligands (calcium complexes of DOTA and DTPA) were compared on this 'sensitized', model of SNx rats fed a high-phosphate diet. Macroscopic (ulcerations and scabs) and histopathological skin lesions were only observed in gadodiamide-treated animals. The other categories of GCs, which are thermodynamically more stable (Port *et al.*, 2008), were not associated with macroscopic or microscopic skin lesions. Furthermore, no lesions were found with the two polyazapolycarboxylic ligands tested, the macrocyclic Ca-DOTA and the linear Ca-DTPA. The daily dose of free ligand selected in this study was consistent with the dose of caldiamide (the free ligand added to the commercial solution of gadodiamide) used in another study (Sieber *et al.*, 2008a).

Bands of dermal inflammatory fibrosis were found in six of the eight gadodiamide-treated rats. Increased cellularity of the dermis was also observed. Interestingly, TGFβ_1 staining was observed on both dermal macrophages and spindle cells. Elevated tissue levels of TGFβ messenger RNA (mRNA) have been previously identified in NSF (Jiménez *et al.*, 2004). Also in another study, an increase in TGFβ protein and mRNA levels and Smad-2 and Smad-3 mRNA levels was reported (Schieren *et al.*, 2010). Positive immunostaining for TGFβ_1 was also demonstrated in NSF skin samples (Kelly *et al.*, 2008) as well as Smad-2 and -3 nuclear staining. These results suggest an association between TGFβ_1 and fibrosis in NSF. TGFβ_1 is a key mediator in fibrosis, as it induces fibroblasts to synthesize and contract the ECM (LeRoy *et al.*, 1990; Schiller *et al.*, 2004). Dermal CD34 expression is an important feature of NSF (Cowper *et al.*, 2008). It is noteworthy that moderate CD34 and S100A4 (i.e. fibroblast-specific protein-1) expression was observed in control biopsy samples. In human skin, CD34 has been demonstrated in vascular endothelial cells, in a subset of dendritic/spindle-shaped cells (Nickoloff, 1991), and in some skin tumours (Cohen *et al.*, 1997). The increased immunostaining of these markers, observed in gadodiamide-

treated rats, reflects the increased density of fibroblasts in the dermis. The CD34+ cells may represent recently migrated CD34+ fibrocytes (bone marrow-derived mesenchymal stem cells) (Bucala, 2008). Moreover, the possibility of CD34+ endothelial cells cannot be ruled out.

P-4-OH is an essential enzyme in collagen synthesis (Gorres and Raines, 2010). P-4-OH-positive foci were exclusively found in the dermis of gadodiamide-treated rats. This finding is consistent with that of another study (Haylor *et al.*, 2010) in which positive immunohistochemical staining for this enzyme was found after a single injection of gadodiamide in renally impaired rats.

Overall, the pathological features observed under these experimental conditions are compatible with those of NSF. However, no α-SMA staining was observed in our model, while α-SMA+ myofibroblasts have been reported in NSF lesions 3 to 4 weeks old (Swartz *et al.*, 2003; Cowper, 2007). However, it is noteworthy that in a recent study (Kelly *et al.*, 2010), NSF skin samples were negative for α-SMA. The same authors reported strong expression of TIMP-1 accompanied by almost absent expression of MMP-1. Another study reported increased levels of expression of both TIMP-1 mRNA and protein in skin samples from NSF patients (Schieren *et al.*, 2010). Under our experimental conditions, TIMP-1 immunostaining was detected on both dermal macrophages and spindle cells. TIMP-1 blocks the activation of MMP-1 (Matrisian, 1990), that plays a pivotal role in collagen degradation. Gadolinium chloride (Bhagavathula *et al.*, 2010) and gadodiamide (DaSilva *et al.*, 2010) have both been shown to stimulate MMP-1 and TIMP-1 production with no apparent increase in type I procollagen production in cultured human skin fibroblasts.

Renal dysfunction is the common predisposing factor of NSF (Cowper, 2007). Several clinical (Thakral *et al.*, 2007; Abraham *et al.*, 2008) and preclinical studies (Pietsch *et al.*, 2009 and Pietsch *et al.*, 2011; Sieber *et al.*, 2008a,b) have demonstrated that Gd may persist in tissues for long periods of time. In our study, no significant differences in plasma total Gd levels were observed in GC-treated rats, except in gadobenate-treated rats, in which lower plasma total Gd concentrations were observed at all time-points. Gadobenate is eliminated in urine and bile (Spinazzi *et al.*, 1999) with intense biliary excretion in rats (50% excretion rate 7 h after injection; Lorusso *et al.*, 1999). As the rats used in the present study were renally impaired, it is likely that biliary clearance of gadobenate was increased to compensate for renal impairment and that total clearance of this compound exceeded that of the other GCs tested (Ersoy and Rybicki, 2007).

The Gd concentrations found in the skin, femur and liver were higher in gadodiamide-treated rats than in the other GC-treated groups. No difference was observed between the two macrocyclic GCs tested, gadoterate and gadobutrol (except in the liver). These results are consistent with those of another study conducted in rats (Sieber *et al.*, 2008b). Preclinical data (Sieber *et al.*, 2008a,b; Pietsch *et al.*, 2009; Steger-Hartmann *et al.*, 2009; Pietsch *et al.*, 2011) are strongly suggestive of a causal role for dissociated Gd^{3+}. *In vivo* dissociation of Gd^{3+} has been found in SNx rats treated with gadodiamide, while no such effect was observed with the macrocyclic GC gadoterate (Fretellier *et al.*, 2011b).

Our data are consistent with the gradual release of Gd from gadodiamide in tissues of treated rats, while no such effect was found with the macrocyclic GCs gadoterate or gadobutrol. A dramatic increase in the r_1 value in liver samples was observed in rats treated with gadobenate. A possible explanation is that gadobenate binds to albumin. The r_1 relaxivity value at 20 MHz of the free contrast agent (without any binding to albumin) ('r_1 free') is 4.5 $mM^{-1}{\cdot}s^{-1}$ and the r_1 value of the non-covalently albumin-bound contrast agent ('r_1 bound') is 36 $mM^{-1}{\cdot}s^{-1}$ (Port *et al.*, 2005). However, in trabecular femur, the increase in the *in vivo* r_1 value was lower than that observed in liver tissue, but higher than that measured *in vitro* in bone matrix, suggesting a possible *in vivo* dissociation of gadobenate in bone tissue. The r_1 value at Day 25 (in skin and bone) could not be determined in 19/25 rats treated with gadobutrol, gadobenate or gadoterate because the $1/T1_{sample} - 1/T1_{diamagnetic}$ value was less than 20% of $1/T1_{diamagnetic}$ (low total Gd concentration in samples).

Hyperphosphataemia probably increases the risk of dissociation of linear GCs in biological milieu. Frenzel *et al.* (2008) showed that Gd^{3+} release rate for non-ionic linear GCs and the total amount released after 15 days were increased in human plasma at 37°C, following addition of 10 mM phosphate, while no effect was observed for macrocyclic GCs. The amount of Gd^{3+} released from gadobenate was substantially lower than that released from non-ionic linear GCs, but higher than that released from macrocyclic agents. Altogether, these results were consistent with the thermodynamic stability range of GCs (Port *et al.*, 2008).

It may be tempting to link the clinical sensitization of the SNx model associated with hyperphosphataemia, observed in Study 1, to phosphate-associated dissociation of gadodiamide and, subsequently, to a profibrosing effect of dissociated Gd. However, the protocol used in our study cannot provide any conclusions concerning this hypothesis, which would require demonstration of a correlation between skin dissociated Gd concentrations and pathological lesions (such as increased cellularity, and/or changes in ECM). However, while relaxometry can be used to detect dissociated states of Gd in solid tissues such as skin or bone, it cannot quantify this dissociation. HPLC-ICP-MS allows quantification of dissociated Gd^{3+} in plasma but cannot be used in solid tissues, in which it would be more pathophysiologically relevant. Therefore, the bioanalytical tools at the present time are unable to correlate dissociated Gd concentration and skin lesions.

The question of which Gd species is actually involved in the pathogenesis of the lesions observed remains unanswered. Several studies have demonstrated micron-sized insoluble deposits containing Gd associated with calcium and phosphate in NSF patients (Thakral and Abraham, 2009; George *et al.*, 2010). The protocol used in our study was unable to distinguish precipitated insoluble Gd in tissues. However, the presence of circulating soluble and probably protein-bound Gd was demonstrated in gadodiamide-treated rats. All states of Gd (i.e. dissociated and soluble, dissociated and precipitated and/or chelated) may be present in the samples. Gadolinium (in the form of $GdCl_3$) has been shown to promote fibroblast proliferation *in vitro* (Varani *et al.*, 2009; Bhagavathula *et al.*, 2010; Edward *et al.*, 2010), an effect associated with the formation of insoluble, Gd and phosphorous-containing aggregated particles (Li *et al.*, 2010).

The release of dissociated Gd from a GC must be estimated by taking into account both the thermodynamic and

kinetic stabilities (Idée *et al.*, 2009). It is speculated that, in the case of low thermodynamic stability but high kinetic stability, the timescale would be too long to reach a biologically significant Gd release in animals. Sensitization of NSF models should accelerate Gd dissociation in order to induce clinically relevant lesions. In our study, hyperphosphataemia sensitized SNx rats to gadodiamide. This is consistent with Frenzel's data showing a phosphate-related dissociation of linear GCs. Nevertheless, in the case of 'intermediate' molecules (i.e. poor thermodynamic stability but high kinetic stability, such as gadobutrol), additional sensitization may be needed to shorten the timescale in order to evaluate their safety under more discriminative conditions.

In conclusion, hyperphosphataemia sensitizes the effects of the linear, non-ionic GC gadodiamide in renally impaired rats. This GC appears to be the most toxic of the commercially available GCs. Further studies are warranted to better understand the mechanism of NSF and the role of hyperphosphataemia as a risk factor.

Acknowledgements

The authors thank Drs Anthony Saul and Dominique Debize-Henderson for reviewing the English version of the manuscript.

Conflicts of interest

All work was funded by Guerbet. NF, JMI, GJ, CF, NP, AD, NB, MP and CC are or were employees of Guerbet.

References

Abraham JL, Thakral C, Skov L, Rossen K, Marckmann P (2008). Dermal inorganic gadolinium concentrations: evidence for in vivo transmetallation and long-term persistence in nephrogenic systemic fibrosis. Br J Dermatol 158: 273–280.

Bhagavathula N, Dame MK, Dasilva M, Jenkins W, Aslam MN, Perone P *et al.* (2010). Fibroblast response to gadolinium: role for platelet-derived growth factor receptor. Invest Radiol 45: 769–777.

Braverman IM, Cowper SE (2010). Nephrogenic systemic fibrosis. F1000 Med Rep 2: 84.

Broome DR (2008). Nephrogenic systemic fibrosis associated with gadolinium based contrast agents: a summary of the medical literature reporting. Eur J Radiol 66: 230–234.

Bucala R (2008). Circulating fibrocytes: cellular basis for NSF. J Am Coll Radiol 5: 36–39.

Cohen PR, Rapini RP, Farhood AI (1997). Dermatopathologic advances in clinical research. The expression of antibody to CD34 in mucocutaneous lesions. off. Dermatol Clin 15: 159–176.

Coladonato JA (2005). Control of hyperphosphataemia among patients with ESRD. J Am Soc Nephrol 16 (Suppl. 2): 107–114.

Cowper SE (2007). Nephrogenic systemic fibrosis: a review and exploration of the role of gadolinium. Adv Dermatol 23: 131–154.

Cowper SE, Su LD, Bhawan J, Robin HS, LeBoit PE (2001). Nephrogenic fibrosing dermopathy. Am J Dermatopathol 23: 383–393.

Cowper SE, Rabach R, Girardi M (2008). Clinical and histological findings in nephrogenic systemic fibrosis. Eur J Radiol 66: 191–199.

Crissman JW, Goodman DG, Hildebrandt PK, Maronpot RR, Prater DA, Riley JH *et al.* (2004). Best practices guideline: toxicologic histopathology. Toxicol Pathol 32: 126–131.

DaSilva M, Deming MO, Fligiel SE, Dame MK, Johnson KJ, Swartz RD *et al.* (2010). Responses of human skin in organ culture and human skin fibroblasts to a gadolinium-based MRI contrast agent: comparison of skin from patients with end-stage renal disease and skin from healthy subjects. Invest Radiol 45: 733–739.

Edward M, Quinn JA, Burden AD, Newton BB, Jardine AG (2010). Effect of different classes of gadolinium-based contrast agents on control and nephrogenic systemic fibrosis-derived fibroblast proliferation. Radiology 256: 735–743.

Ersoy H, Rybicki FJ (2007). Biochemical safety profiles of gadolinium-based extracellular contrast agents and nephrogenic systemic fibrosis. J Magn Reson Imaging 26: 1190–1197.

Frenzel T, Lengsfeld P, Schirmer H, Hütter J, Weinmann HJ (2008). Stability of gadolinium-based magnetic resonance imaging contrast agents in human serum at 37°C. Invest Radiol 73: 817–828.

Fretellier N, Idée JM, Guerret S, Hollenbeck C, Hartmann D, González W *et al.* (2011a). Clinical, biological, and skin histopathological effects of ionic macrocyclic and nonionic linear gadolinium chelates in a rat model of nephrogenic systemic fibrosis. Invest Radiol 46: 85–93.

Fretellier N, Idée JM, Dencausse A, Karroum O, Guerret S, Poveda N *et al.* (2011b). comparative in vivo dissociation of gadolinium chelates in renally impaired rats: a relaxometry study. Invest Radiol 46: 292–300.

George SJ, Webb SM, Abraham JL, Cramer SP (2010). Synchrotron X-ray analyses demonstrate phosphate-bound gadolinium in skin in nephrogenic systemic fibrosis. Br J Dermatol 163: 1077–1081.

Gorres KL, Raines RT (2010). Prolyl 4-hydroxylase. Crit Rev Biochem Mol Biol 45: 106–124.

Grant D, Johnsen H, Juelsrud A, Løvhaug D (2009). Effects of gadolinium contrast agents in naïve and nephrectomised rats: relevance to nephrogenic systemic fibrosis. Acta Radiol 50: 156–169.

Grobner T (2006). Gadolinium: a specific trigger for the development of nephrogenic fibrosing dermopathy and nephrogenic systemic fibrosis? Nephrol Dial Transplant 21: 1104–1108.

Haylor J, Dencausse A, Vickers M, Nutter F, Jestin G, Slater D *et al.* (2010). Nephrogenic gadolinium biodistribution and skin cellularity following a single injection of Omniscan in the rat. Invest Radiol 45: 507–512.

Idée JM, Port M, Robic C, Medina C, Sabatou M, Corot C (2009). Role of thermodynamic and kinetic parameters in gadolinium chelate stability. J Magn Reson Imaging 30: 1249–1258.

Jiang Y, Wang M (2008). Hyperphosphataemia-induced hyperparathyroidism in 5/6 nephrectomized rats: development of a new animal model. Chin Med J 121: 2440–2443.

Jiménez SA, Artlett CM, Sandorfi N, Derk C, Latinis K, Sawaya H *et al.* (2004). Dialysis-associated systemic fibrosis (nephrogenic fibrosing dermopathy): study of inflammatory cells and transforming growth factor beta1 expression in affected skin. Arthritis Rheum 50: 2660–2666.

Kelly B, Petitt M, Sanchez R (2008). Nephrogenic systemic fibrosis is associated with transforming growth factor beta and Smad without evidence of renin-angiotensin system involvement. J Am Acad Dermatol 58: 1025–1030.

Kelly BC, Markle LS, Vickers JL, Petitt MS, Raimer SS, McNeese C (2010). The imbalanced expression of matrix metalloproteinases in nephrogenic systemic fibrosis. J Am Acad Dermatol 63: 483–489.

LeRoy EC, Trojanowska MI, Smith EA (1990). Cytokines and human fibrosis. Eur Cytokine Netw 1: 215–219.

Li JX, Liu JC, Wang K, Yang XG (2010). Gadolinium-containing bioparticles as active antity to promote cell cycle progression in mouse embryo fibroblast NIH3T3 cells. J Biol Inorg Chem 15: 547–557.

Lorusso V, Arbughi T, Tirone P, de Haën C (1999). Pharmacokinetics and tissue distribution in animals of gadobenate ion, the magnetic resonance imaging contrast enhancing component of gadobenate dimeglumine 0.5 M solution for injection (MultiHance). J Comput Assist Tomogr 23 (Suppl. 1): 181–194.

Mahl A, Heining P, Ulrich P, Jakubowski J, Bobadilla M, Zeller W *et al*. (2000). Comparison of clinical pathology parameters with two different blood sampling techniques in rats: retrobulbar plexus versus sublingual vein. Lab Anim 34: 351–361.

Marckmann P, Skov L, Rossen K, Heaf JG, Thomsen HS (2007). Case-control study of gadodiamide-related nephrogenic systemic fibrosis. Nephrol Dial Transplant 22: 3174–3178.

Matrisian LM (1990). Metalloproteinases and their inhibitors in matrix remodeling. Trends Genet 6: 121–125.

Nickoloff BJ (1991). The human progenitor cell antigen (CD34) is localized on endothelial cells, dermal dendritic cells, and perifollicular cells in formalin-fixed normal skin, and on proliferating endothelial cells and stromal spindle-shaped cells in Kaposi's sarcoma. Arch Dermatol 127: 523–529.

Oste L, Behets GJ, Dams G, Bervoets AR, Marynissen RL, Geryl H *et al*. (2007). Role of dietary phosphorus and degree of uremia in the development of renal bone disease in rats. Ren Fail 29: 1–12.

Peak A, Sheller A (2007). Risk factors for developing gadolinium-induced nephrogenic systemic fibrosis. Ann Pharmacother 41: 1481–1485.

Perazella MA, Reilly RF (2011). Imaging patients with kidney disease: how do we approach contrast-related toxicity? Am J Med Sci 341: 215–221.

Pietsch H, Lengsfeld P, Steger-Hartmann T, Löwe A, Frenzel T, Hütter J *et al*. (2009). Impact of renal impairment on long-term retention of gadolinium in the rodent skin following the administration of gadolinium-based contrast agents. Invest Radiol 44: 226–233.

Pietsch H, Raschke M, Ellinger-Ziegelbauer H, Jost G, Walter J, Frenzel T *et al*. (2011). The role of residual gadolinium in the induction of nephrogenic systemic fibrosis-like skin lesions in rats. Invest Radiol 46: 48–56.

Port M, Corot C, Violas X, Robert P, Raynal I, Gagneur G (2005). How to compare the efficiency of albumin-bound and nonalbumin-bound contrast agents in vivo: the concept of dynamic relaxivity. Invest Radiol 40: 565–573.

Port M, Idée JM, Medina C, Robic C, Sabatou M, Corot C (2008). Efficiency, thermodynamic and kinetic stability of marketed gadolinium chelates and their possible clinical consequences: a critical review. Biometals 21: 469–490.

Prince MR, Zhang H, Morris M, MacGregor JL, Grossman ME, Silberzweig J *et al*. (2008). Incidence of nephrogenic systemic fibrosis at two large medical centers. Radiology 248: 807–816.

Sanchez CP, He YZ, Leiferman E, Wilsman NJ (2004). Bone elongation in rats with renal failure and mild or advanced secondary hyperparathyroidism. Kidney Int 65: 1740–1748.

Schieren G, Gambichler T, Skrygan M, Burkert B, Altmeyer P, Rump LC *et al*. (2010). Balance of profibrotic and antifibrotic [corrected] signaling in nephrogenic systemic fibrosis skin lesions. Am J Kidney Dis 55: 1040–1049.

Schiller M, Javelaud D, Mauviel A (2004). TGF-beta-induced SMAD signaling and gene regulation: consequences for extracellular matrix remodeling and wound healing. J Dermatol Sci 35: 83–92.

Sieber MA, Pietsch H, Walter J, Haider W, Frenzel T, Weinmann HJ (2008a). A preclinical study to investigate the development of nephrogenic systemic fibrosis: a possible role for gadolinium-based contrast media. Invest Radiol 43: 65–75.

Sieber MA, Lengsfeld P, Frenzel T, Golfier S, Schmitt-Willich H, Siegmund F *et al*. (2008b). Preclinical investigation to compare different gadolinium-based contrast agents regarding the propensity to release gadolinium in vivo and to trigger nephrogenic systemic fibrosis-like lesions. Eur Radiol 18: 2164–2173.

Spinazzi A, Lorusso V, Pirovano G, Kirchin M (1999). Safety, tolerance, biodistribution, and MR imaging enhancement of the liver with gadobenate dimeglumine: results of clinical pharmacologic and pilot imaging studies in nonpatient and patient volunteers. Acad Radiol 6: 282–291.

Steger-Hartmann T, Raschke M, Riefke B, Pietsch H, Sieber MA, Walter J (2009). The involvement of pro-inflammatory cytokines in nephrogenic systemic fibrosis. A mechanistic hypothesis based on preclinical results from a rat model treated with gadodiamide. Exp Toxicol Pathol 61: 537–552.

Swartz RD, Crofford LJ, Phan SH, Ike RW, Su LD (2003). Nephrogenic fibrosing dermopathy: a novel cutaneous fibrosing disorder in patients with renal failure. Am J Med 114: 563–572.

Thakral C, Abraham JL (2009). Gadolinium-induced nephrogenic systemic fibrosis is associated with insoluble Gd deposits in tissues: in vivo transmetallation confirmed by microanalysis. J Cutan Pathol 36: 1244–1254.

Thakral C, Alhariri J, Abraham JL (2007). Long-term retention of gadolinium in tissues from nephrogenic systemic fibrosis patient after multiple gadolinium-enhanced MRI scans: case report and implications. Contrast Media Mol Imaging 2: 199–205.

US Food and Drugs Administration CfDEaR (2005). Guidance for industry. Estimating the maximum safe starting dose in initial clinical trials for therapeutics in adult healthy volunteers. http://www.fda.gov/downloads/Drugs/GuidanceCompliance RegulatoryInformation/Guidances/ucm078932.pdf%202005:1-27 (last accessed 29 March 2011).

Vakil V, Sung JJ, Piecychna M, Crawford JR, Kuo P, Abu Alfa AK *et al*. (2009). Gadolinium-containing magnetic resonance image contrast agents promotes fibrocytes differentiation. J Magn Reson Imaging 20: 1284–1288.

Varani J, DaSilva M, Warner RL, Deming MO, Barron AG, Johnson KJ (2009). Effects of gadolinium-based magnetic resonance imaging contrast agents on human skin in organ culture and human skin fibroblasts. Invest Radiol 44: 74–81.

Wilford C, Fine JD, Boyd AS, Sanyal S, Abraham JL, Kantrow SM (2010). Nephrogenic systemic fibrosis: report of an additional case with granulomatous inflammation. Am J Dermatopathol 32: 71–75.